


Making Bright Giants Invisible At The Galactic Centre

Pau Amaro-Seoane¹ ^{*}, Xian Chen², Rainer Schödel³ & Jordi Casanellas⁴

¹ *Institute of Space Sciences (ICE, CSIC) & Institut d'Estudis Espacials de Catalunya (IEEC)*

at Campus UAB, Carrer de Can Magrans s/n 08193 Barcelona, Spain

Kavli Institute for Astronomy and Astrophysics, Beijing 100871, China

Institute of Applied Mathematics, Academy of Mathematics and Systems Science, CAS, Beijing 100190, China

Zentrum für Astronomie und Astrophysik, TU Berlin, Hardenbergstraße 36, 10623 Berlin, Germany

² *Astronomy Department, School of Physics, Peking University, 100871 Beijing, China*

Kavli Institute for Astronomy and Astrophysics, Peking University, Beijing 100871, China

(Corresponding author.)

³ *Instituto de Astrofísica de Andalucía, Glorieta de la Astronomía s/n, 18008 Granada, Spain*

⁴ *DataGuda, Septimania 41, Barcelona, Spain*

draft 11 November 2020

ABSTRACT

Current observations of the Galactic Center (GC) seem to display a core-like distribution of bright stars from $\sim 5''$ inwards. On the other hand, we observe young, massive stars at the GC, with roughly 20-50% of them in a disc, mostly in the region where the bright giants appear to be lacking. In a previous publication we put the idea forward that the missing stars are deeply connected to the presence of this disc. The progenitor of the stellar disc is very likely to have been a gaseous disc that at some point fragmented and triggered star formation. This caused the appearance of overdensity regions in the disc that had high enough densities to ensure stripping large giants of their atmospheres and thus rendering them very faint. In this paper we use a stellar evolution code to derive the properties that a red giant would display in a colour-magnitude diagram, as well as a non-linearity factor required for a correct estimate of the mass loss. We find that in a very short timescale, the red giants (RGs) leave their standard evolutionary track. The non-linearity factor has values that not only depend on the properties of the clumps, but also on the physical conditions the giant stars, as we predicted analytically. According to our results, envelope stripping works, moving stars on a short timescale from the giant branch to the white dwarf stage, thus rendering them invisible to observations.

Key words: a keyword – another.

1 INTRODUCTION

Stellar dynamics predicts that the stars inside the influence radius of a supermassive black hole (SMBH) will relax in the energy and angular-momentum space to form a cuspy distribution with the stellar density increasing towards the SMBH (Peebles 1972; Bahcall & Wolf 1976; Amaro-Seoane et al. 2004; Freitag et al. 2006; Alexander & Hopman 2009; Preto & Amaro-Seoane 2010; Amaro-Seoane & Preto 2011; Amaro-Seoane 2018).

These theoretical findings have been thought to contradict observations of the GC, which seemed to show that the surface density of bright stars¹ within a distance of 0.5 pc

from the SMBH Sgr A* is constant (“core-like”) if not decreasing towards the SMBH (“hole-like” Genzel et al. 1996; Buchholz et al. 2009; Do et al. 2009; Yusef-Zadeh et al. 2012). However, recently, the works of Gallego-Cano et al. (2018) and Schödel et al. (2018) have addressed the observational data at the GC with an improved methodology which allowed them to obtain star counts for fainter stars than in previous works and to obtain the surface brightness profile of the diffuse stellar light. As a result of their analysis, they find that the stellar density can be described by a three-dimensional power-law with an exponent value of ≈ -1.2 . Remarkably, these results are in very good agreement with the numerical work of Baumgardt et al. (2018). However, they also confirm the lack of bright giants within ~ 0.2 pc of SgrA*. Also, the work of Habibi et al. (2019) finds a cusp in the old giants population within 0.02 – 0.4 pc.

Several dynamical processes have been proposed to explain the difference of the distribution of red giants (RGs)

^{*} E-mail: pau@ice.cat (PAS)

¹ In this context, “bright” refers to giant stars as luminous or more luminous as Red Clump stars, which have an observed extinguished K magnitude at the GC of about 15-16.

from other stars. It was suggested that collisions with main-sequence stars could reduce the density of RGs (Genzel et al. 1996), but later calculations showed that the resulting size of the core-like nucleus would be too small to explain the observations (Davies et al. 1998; Alexander 1999; Bailey & Davies 1999; Dale et al. 2009). More recently, it was found that the collision of RGs with dense gas clumps in a star-forming gaseous disc, such as the one that formed the observed stellar disc in our GC, could more efficiently destroy RGs and reproduce the core size (see Amaro-Seoane & Chen 2014, “Paper I” from now onwards). Compared to main-sequence, RGs have larger sizes and lower surface gravity, and hence are more susceptible to mass loss during such a collision (see Armitage et al. 1996, who addressed this from a numerical standpoint in the context of homogeneous discs). Moreover, the amount of mass that is lost grows exponentially if the collision repeats (“non-linearity”), because after each collision a RG inflates and the self-gravity of the outer envelope decreases (as explained in Paper I, but see as well Armitage et al. 1996; Kieffer & Bogdanovic 2016). The condition in the GC is favorable to multiple collisions, as explained in Paper I, because in the central 0.5 pc are ~ 200 massive young stars (Genzel et al. 2010), indicating that at least an equal amount of gas clouds had existed in the past².

In Paper I we presented the idea of how to make giant stars invisible at the GC. Due to the limitations of the analytical calculations, a few questions remain open: (i) a RG which has lost a significant amount of its envelope could become brighter, or dimmer, depending on its evolutionary stage (Dray et al. 2006). This means that RG-cloud collisions do not necessarily remove RGs from the sensible range of a telescope, and hence this not necessarily solves the aforementioned “missing RG problem”; (ii) Addressing this issue requires calculation of the evolution tracks of RGs in the Hertzsprung-Russell diagram (pointed out by Kieffer & Bogdanovic 2016); (iii) The estimation of the non-linearity factor f , necessary to calculate the mass loss per hit, is difficult, if not impossible, to derive from first principles and (iv) the properties of the released degenerate cores were not addressed in Paper I.

2 METHOD

In this section we present the algorithm to calculate the partial removal of the envelope of a bright giant after hitting a clump, which is the scenario presented in Paper I, as well as the numerical stellar code and the implementation of the mass loss in it.

2.1 Mass loss during collisions

When a red giant (RG) collides with a gas clump of surface density Σ_c and mass M_c at a relative velocity of v_c , only that part of the envelope satisfying the condition

² Kieffer & Bogdanovic (2016) found that multiple collisions are unlikely. This is due to a very small cloud size they derived from a thin accretion-disc model. But observations indicate that the accretion disc is mildly thick, so that the resulting cloud size is much larger (see Paper I for the derivation).

$$\Sigma_*(R)\sqrt{\frac{GM_*(R)}{R}} < \Sigma_c v_c \quad (1)$$

will be stripped off the RG (Armitage et al. 1996). Here, $\Sigma_*(R)$ is the surface density (see below for derivation) of the RG as a function of stellar radius R , and $M_*(R)$ is the mass enclosed inside R . For a collision happening at a distance D from the Sgr A*, $v_c \simeq 400[D/(0.1 \text{ pc})]^{-1/2} \text{ km s}^{-1}$. In the following we adapt $v_c = 400 \text{ km s}^{-1}$ as a fiducial value for our simulations.

Following the analysis presented in Paper I, and using the same notation, we calculate Σ_c with

$$\Sigma_c \simeq 2 \cdot 10^4 \text{ g cm}^{-2} \left(\frac{M_c}{10^2 M_\odot}\right)^{-1} \left(\frac{D}{0.1 \text{ pc}}\right)^{-2} \left(\frac{H}{0.1 D}\right)^4. \quad (2)$$

Assuming that the accretion disc which created the clumps has a geometric thickness of $H/D = 0.1$ and the typical mass of the clumps is $10^2 M_\odot$, we estimate that $\Sigma_c = 2 \cdot 10^4 \text{ g cm}^{-2}$ for a clump at $D = 0.1 \text{ pc}$. For these parameters, the size of the clumps is typically $R_c \sim 10^{-2} D$. Given that today there are about 10^2 massive stars in the observed young stellar disc in the GC, the total mass of the disk is about $10^4 M_\odot$, which is also consistent with the mass of the disc required by the dynamical model to explain the distribution of the other young stars (e.g., S-stars) in the GC (Chen & Amaro-Seoane 2014).

The mass loss during one collision, ΔM , is calculated as follows with Equation (1):

(i) Derive the function $M_*(R)$ from the output of the stellar evolution model. If not in the output, calculate it using the density $\rho_*(r)$ of the RG,

$$M_*(R) = 4\pi \int_0^R \rho_*(r)r^2 dr. \quad (3)$$

(ii) Derive $\Sigma_*(R)$ for any $0 < R < R_*$, where R_* is the radius of the RG,

$$\Sigma_*(R) = 2 \int_0^{\sqrt{R_*^2 - R^2}} \rho(\sqrt{h^2 + R^2}) dh. \quad (4)$$

(iii) Find the critical radius R_s , such that Equation (1) is satisfied when $R > R_s$.

(iv) The stellar mass at $R > R_s$ that will be stripped off the RG during the collision, is therefore

$$\Delta M = M_*(R_*) - M_*(R_s). \quad (5)$$

2.2 Implementation in a stellar evolution code

We implement this mechanism of mass loss in the stellar evolution code CESAM (Morel & Lebreton 2008). The code allows one to compute stellar models from the pre-main sequence phase to advanced stages. It has been widely used in the context of asteroseismic studies (Stello et al. 2009) and in particular to simulate red-giant stars (Mosser et al. 2012; Piau et al. 2011).

We modify the original subroutines for external, constant mass loss to include the mass loss due to repeated collisions with a gas clump. For each collision, we solve Equations 1, 4 and 5 to find the critical radius R_s above which all mass is stripped from the star. The amount of mass lost in each collision, ΔM , is spread over a time span of 10^3 yr to guarantee the convergence of the code in the face of the strong structural variations that occur when the envelope is stripped.

We simulate the evolution through the red giant branch of stars from $M_\star = 1 M_\odot$ to $7 M_\odot$ (note that that high masses are of interest to also consider recent star formation; for a population older than 1 (3) Gyr, it is enough to consider masses < 3 (2) M_\odot). We then consider collisions with gas clumps with surface densities from $\Sigma_c = 10^4 \text{ g cm}^{-2}$ to 10^6 g cm^{-2} . The collisions with the gas clumps start when the stars evolve through the red giant branch, once they reach radii ranging from $R_{\star,i} = 30 R_\odot$ to $100 R_\odot$. After removing the mass lost in one collision, we let the stars evolve during $5 \cdot 10^4$ yr without any mass loss before undergoing another collision. This treatment leads to 20 collisions in every 1 Myr, to be consistent with the estimations in Paper I. The time during which the stars experience multiple collisions depends on the timescale of the fragmenting phase of the stellar disc, which in turn depends on the lifetime of the clumps. In Paper I we found that the typical lifetime is 10^5 years but for less massive clumps (i.e., denser clumps according to Eq. 2) the lifetime could be as long as a few Myrs. Therefore, we vary the collision time between 0.4 and 5 Myrs.

3 RESULTS

In Figure 1 we depict the evolution of the stellar masses and radii for red giants as a function of the number of accumulated hits with clumps. The larger the radius, the more efficient the removal of mass from the envelope is. Obviously, the more massive the star is, the longer it takes to achieve a significant mass loss. The figure also shows that during the first collisions, the loss of the envelop leads to an expansion of the stellar radius. The expansion is caused by the higher gas pressure in the deeper part of the envelope. When almost all the envelope is removed, the star stops to expand and shrinks after each collision.

In Figure 2 we show the evolution of the RGs in the Hertzsprung-Russell (HR) diagram. In general, a RG becomes brighter and cooler during the first tens of collisions, as a result of the expansion of the stellar radius. When almost all the envelope is removed, the evolutionary track turns horizontally: The star becomes hotter in successive collisions while the bolometric luminosity remains constant.

After leaving the standard track for RGs, the remnant of the RG quickly cools and settles down on the white-dwarf branch, as is shown in Figure 3. White dwarfs are too faint to be detected at the GC with current instrumentation. Thus, a RG will become “invisible” after envelope stripping.

Using the above method, for each collision we derive the amount of mass ΔM that is lost from the RG envelope. We denote the mass loss during the n th collision as ΔM_n ($n \geq 1$), and for each collision we calculate the non-linearity factor with $f = \Delta M_{n+1} / \Delta M_n$. The bigger the non-linearity factor

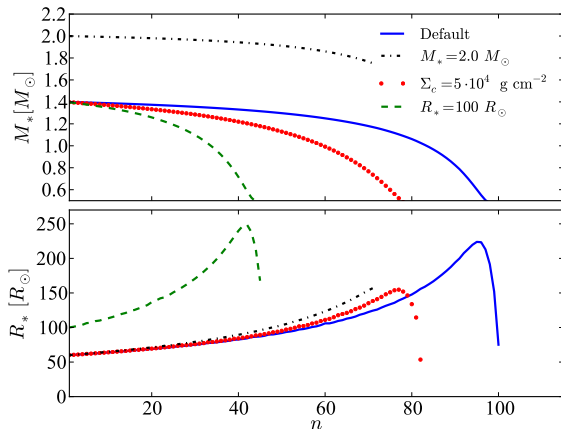


Figure 1. Evolution of the mass M_\star (upper panel) and the radius of the star R_\star (lower panel) as a function of the number of hits n with the clumps in the star-forming disc. The model parameters by default are $M_\star = 1.4 M_\odot$, $R_\star = 60 R_\odot$ and $\Sigma_c = 2 \times 10^4 \text{ g cm}^{-2}$, unless mentioned otherwise in the legend.

is, the smaller number of collisions are needed to remove the envelope of RGs. Numerical simulations with large RGs (with a size of $150 R_\odot$) suggests that f is 2 (Armitage et al. 1996). The value decreases if the size of a RG is smaller. Figure 4 summarizes the results from our simulations: In general $f - 1 = \mathcal{O}(0.1)$, as we estimated in Paper I. The value of f increases with n because of the binding energy of the star decreases.

4 CONCLUSIONS

Previous observations of giant stars as luminous or more luminous as Red Clump stars at the Galactic Center appear to indicate a core-like distribution, and it is important to note that we cannot say whether this also holds for the fainter stars, such as main sequence stars. More recent observations, though, reconcile with theory and numerical simulations (Gallego-Cano et al. 2018; Schödel et al. 2018; Baumgardt et al. 2018). Habibi et al. (2019) confirm the results of Gallego-Cano et al. (2018) and Schödel et al. (2018) that there is a cusp of faint giants ($K_s > 15$). However, this does not change the basic observation that we are missing bright giants.

Theoretically, as explained in the introduction, the missing RGs poses a problem that has been studied for more than 15 years. In Paper I, Amaro-Seoane & Chen (2014), we proposed that the only scenario that could lead to an efficient depletion of the RGs in the GC is the collision of the giant stars with the clumps that later become the observed stellar disc. Although our analytical approach provided a solution to the problem, a few open questions remained, including the features of the giant stars in the colour-magnitude diagram as they suffer consecutive hits with the high-density clumps, and the non-linearity factor that determines the lifetime of the RGs.

In this paper we address the evolution of a giant star in the GC with a numerical stellar evolution code which we have modified to take into account the mass loss due to re-

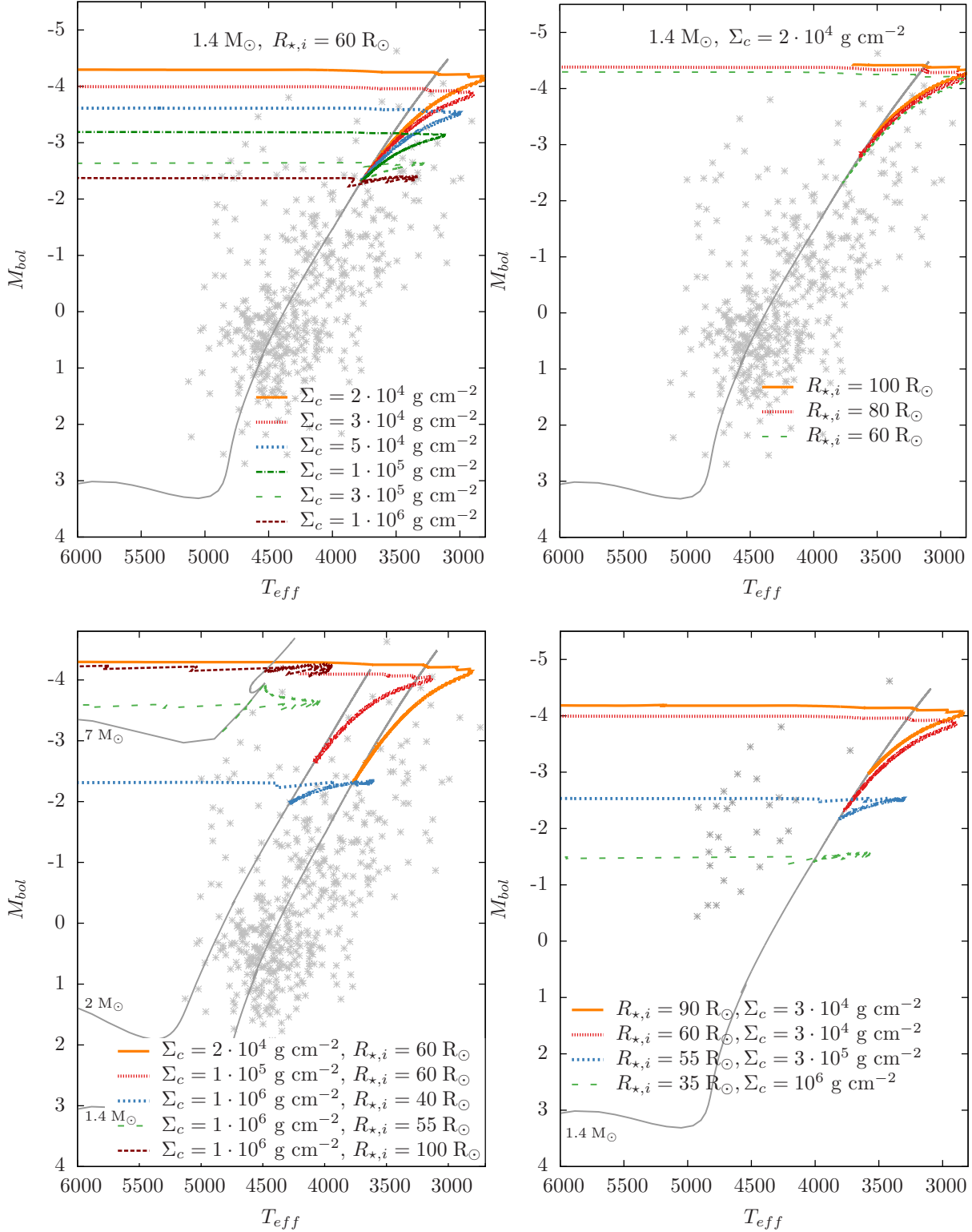


Figure 2. Hertzsprung-Russell (HR) diagram (Bolometric magnitude M_{bol} against effective temperature T_{eff}) for different bright giants and properties of the clumps, including (a) a fixed mass and radius of the star and six different surface densities of the clumps (top left), (b) a fixed mass and surface density and three different stellar radii (top right), (c) three different initial masses, four different surface densities (lower left) and (d) one initial stellar mass, four different initial stellar radii and three different surface densities (lower right). The gray solid curves show the standard evolutionary tracks of RGs, and the colored curves are derived from our model which includes the collisions between RGs and gas clumps. The asterisk symbols show the distribution of RGs in the GC (Ref. here).

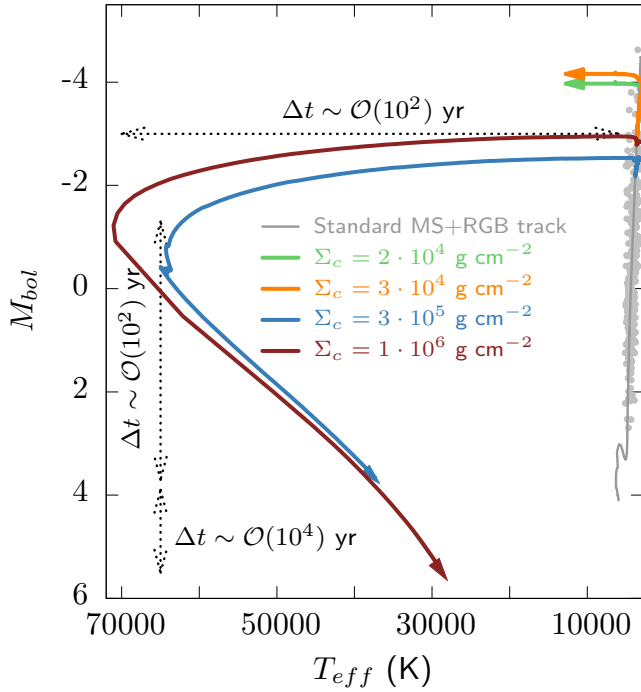


Figure 3. Same HR diagram as in Figure 2 but for much higher temperatures. We depict the evolutionary track of a $1.4 M_{\odot}$ and $60 R_{\odot}$ star after successive impacts with clumps of different surface densities. In grey, to the right, we have the same standard MS+RGB track displayed in the aforementioned Figure. From the “first Knee Point” (see text) to the maximum effective temperatures reached, the evolution happens in very short timescales, of order $\sim 10^2$ yrs. From the “second Knee Point” to the end of the evolution, going back to lower effective temperatures, the timescale, while longer than the previous one, is still short, of order $\sim 10^4$ yrs.

peated hits against a gas clump. We find that clumps remove the envelopes very efficiently. In a very short timescale, the RGs leave their standard evolutionary track and in some 10^5 years move to effective temperatures as high as 70,000K and drop their bolometric magnitude by many orders of magnitude. While this works out very well for RGs, horizontal branch (HB) stars have an envelope 100 times denser in surface density, and consequently require about 100 more impacts to be depleted. As explained in Paper I, this means that most of the HB stars will suffer a partial depletion and only a fraction (those with low inclinations) will have received a significant envelope damage.

We deem it important to stress that (i) we rely on a single episode of disc formation, but it is likely that many episodes have happened, which would help to completely destroy all envelopes, (ii) we assume a population of only 100 clumps, because that is the number of stars that we currently observe in the stellar disc at the GC, although this is a very conservative lower limit. Having more clumps obviously helps in the removal of the envelopes as well and (iii) we consider a single mass ($10^2 M_{\odot}$) for the clumps, while a broad spectrum is more realistic. Having less massive clumps helps in the process of removal of RG envelope, because the surface density of a clump is inversely proportional to its mass (Paper I).

Our theory predicts that giant stars are “hiding”: While

we cannot see them, their degenerate cores are populating the GC, building the old, segregated cusp that a number of independent studies have predicted theoretically.

ACKNOWLEDGMENTS

PAS acknowledges support from the Ramón y Cajal Programme of the Ministry of Economy, Industry and Competitiveness of Spain, as well as the COST Action GW-verse CA16104. This work was supported by the National Key R&D Program of China (2016YFA0400702) and the National Science Foundation of China (11721303 and 11873022). He is indebted with Marta Masini and Luisa Seoane for their encouragement and countless hours of remote support during his visit to the KIAA in Beijing. The research leading to these results has received funding from the European Research Council under the European Union’s Seventh Framework Programme (FP7/2007-2013) / ERC grant agreement nr 614922. RS acknowledges financial support from the State Agency for Research of the Spanish MCIU through the “Center of Excellence Severo Ochoa” award for the Instituto de Astrofísica de Andalucía (SEV-2017-0709). RS acknowledges financial support from the national grant PGC2018-095049-B-C21 (MCIU/AEI/FEDER, UE).

REFERENCES

- Alexander T., 1999, 527, 835
- Alexander T., Hopman C., 2009, ApJ, 697, 1861
- Amaro-Seoane P., 2018, Living Reviews in Relativity, 21, 4
- Amaro-Seoane P., Chen X., 2014, ApJ, 781, L18
- Amaro-Seoane P., Freitag M., Spurzem R., 2004
- Amaro-Seoane P., Preto M., 2011, Classical and Quantum Gravity, 28, 094017
- Armitage P. J., Zurek W. H., Davies M. B., 1996, ApJ, 470, 237
- Bahcall J. N., Wolf R. A., 1976, ApJ, 209, 214
- Bailey V. C., Davies M. B., 1999, MNRAS, 308, 257
- Baumgardt H., Amaro-Seoane P., Schödel R., 2018, 609, A28
- Buchholz R. M., Schödel R., Eckart A., 2009, A&A, 499, 483
- Chen X., Amaro-Seoane P., 2014, ApJ, 786, L14
- Dale J. E., Davies M. B., Church R. P., Freitag M., 2009, MNRAS, 393, 1016
- Davies M. B., Blackwell R., Bailey V. C., Sigurdsson S., 1998, MNRAS, 301, 745
- Do T., Ghez A. M., Morris M. R., Lu J. R., Matthews K., Yelda S., Larkin J., 2009, ApJ, 703, 1323
- Dray L. M., King A. R., Davies M. B., 2006, MNRAS, 372, 31
- Freitag M., Amaro-Seoane P., Kalogera V., 2006, ApJ, 649, 91
- Gallego-Cano E., Schödel R., Dong H., Noguera-Lara F., Gallego-Calvente A. T., Amaro-Seoane P., Baumgardt H., 2018, 609, A26
- Genzel R., Eisenhauer F., Gillessen S., 2010, Reviews of Modern Physics, 82, 3121

- Genzel R., Thatte N., Krabbe A., Kroker H., Tacconi-Garman L. E., 1996, *ApJ*, 472, 153
- Habibi M., Gillessen S., Pfuhl O., Eisenhauer F., Plewa P. M., von Fellenberg S., Widmann F., Ott T., Gao F., Waisberg I., Bauböck M., Jimenez-Rosales A., Dexter J., de Zeeuw P. T., Genzel R., 2019, *ApJ*, 872, L15
- Kieffer T. F., Bogdanovic T., 2016, arXiv:1602.03527
- Morel P., Lebreton Y., 2008, *Astrophysics and Space Science*, 316, 61
- Mosser B., Goupil M. J., Belkacem K., Michel E., Stello D., Marques J. P., Elsworth Y., Barban C., Beck P. G., Bedding T. R., De Ridder J., García R. A., Hekker S., Kallinger T., Samadi R., Stumpe M. C., Barclay T., Burke C. J., 2012, *Astronomy and Astrophysics*, 540, A143
- Peebles P. J. E., 1972, *ApJ*, 178, 371
- Piau L., Kervella P., Dib S., Hauschildt P., 2011, *Astronomy and Astrophysics*, 526, A100
- Preto M., Amaro-Seoane P., 2010, 708, L42
- Schödel R., Gallego-Cano E., Dong H., Noguera-Lara F., Gallego-Calvente A. T., Amaro-Seoane P., Baumgardt H., 2018, 609, A27
- Stello D., Chaplin W. J., Bruntt H., et al. 2009, *The Astrophysical Journal*, 700, 1589
- Yusef-Zadeh F., Arendt R., Bushouse H., Cotton W., Haggard D., Pound M. W., Roberts D. A., Royster M., Wardle M., 2012, *ApJ*, 758, L11

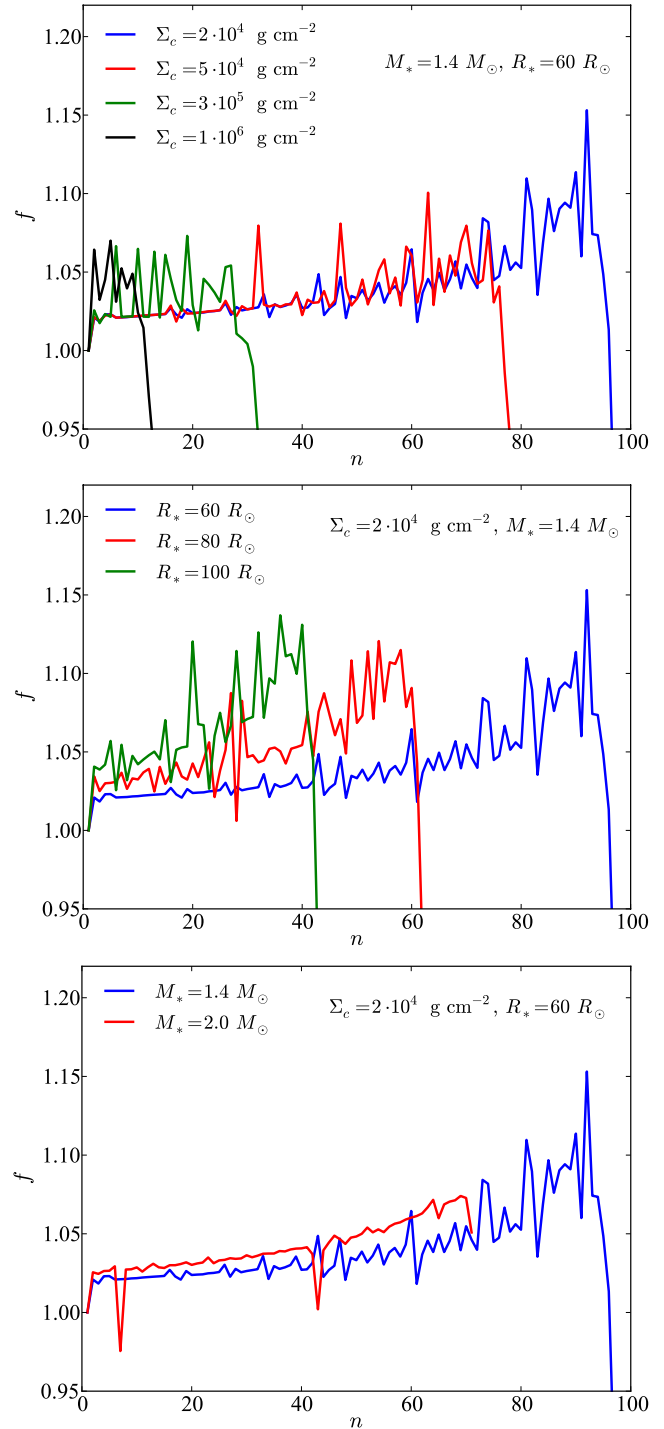


Figure 4. The non-linearity factor, as introduced in Paper I, for four different surface densities and a fixed stellar mass and radius (upper panel), three different initial stellar radii, a fixed surface density and stellar mass (mid panel) and a fixed surface density and stellar radius and two different initial stellar masses (lower panel).